2015 IEEE/RSJ International Conference on Intelligent Robots and Systems (IROS)
Congress Center Hamburg
Sept 28 - Oct 2, 2015. Hamburg, Germany

Power and Endurance Modelling of Battery-Powered Rotorcraft

Analiza Abdilla[1], Arthur Richards[2] and Stephen Burrow[3]
Department of Aerospace Engineering, University of Bristol, UK
Bristol Robotics Laboratory, Bristol, UK

Abstract— **This paper characterises the power consumption of electric rotorcraft and derives an endurance estimation model for such aircraft powered by LiPo batteries. Theoretical analysis is backed by experimental flight tests using a popular commercial quadrotor.**

Experiments on Commercial Off-The-Shelf Lithium-Polymer batteries, which are the technology dominating the multi-rotor Unmanned Aerial Vehicle market, are carried out to determine battery run-time and specific energy/capacity models, whilst investigating the battery variability. These battery models are combined with the rotorcraft power model to provide an endurance estimation model, accounting for both battery variability as well as the electric propulsion system effects, which is experimentally validated through flight tests.

I. INTRODUCTION

Rotary wing Unmanned Aerial Vehicles (UAVs) are widely used in exploration missions due to their hovering and low-speed flight capabilities and high manoeuvrability. However, they suffer from high power consumption as compared with other wing configurations. Such aircraft are available with various number of rotors and/or configurations, with a higher number of rotors resulting in increased payload capability at the cost of higher power consumption, and thus endurance [1]. With severe SWAP (Size, Weight and Power) constraints, the hobby UAV market is dominated by LiPo batteries, which offer the optimal compromise of moderate specific energy, high specific power and high cycle life [2].

This paper characterises the power consumption of electric rotorcraft and derives an endurance estimation model for such aircraft powered by LiPo batteries. The motivation behind this is its use in endurance optimisation of battery-powered rotorcraft, which may be achieved by subdividing the monolithic battery into multiple smaller capacity batteries which are discharged and deployed as required, as described in [3]. The test vehicle utilised for this purpose is the ARDrone2.0 [4], a hobby-grade quadrotor released by Parrot in 2012, which is widely used for both hobby flight and as a research platform due to its ease of use. The approach and principles of the model should however be applicable to any battery-powered multi-rotor UAV.

In literature, such as [2], [5]–[8], endurance is typically estimated as the ratio of the energy available and power consumed. The rotorcraft power is derived based on the rotor hover power from Momentum Theory [9], with the overall efficiency of the mechanical/electrical power conversion termed the propulsion system efficiency, as in [2], [5]–[8], [10]–[13]. This term characterises the individual rotor Figure of Merit, that is, motor, gearbox and propeller combination, as well as the interaction between rotors [9]. Although the propulsion system efficiency increases with increasing rpm, as presented in [2], [12], [13], a constant value is generally adopted, as in [5]–[8], [10], [11].

The battery energy is typically estimated based on a constant Specific Energy/Gravimetric Energy Density for the particular battery technology, which is the energy per unit mass, as in [5], [6], [8], [10], [11], [13], [14]. Besides the battery chemistry, this also depends on the battery packaging and design, as well as the operating point [15]. The Specific Energy of LiPo's varies between 100-300Wh/kg [16], with a value of $\sim$150Wh/kg being typically adopted, as in [5] and [12]. Based on experimental results with Commercial Off-The-Shelf (COTS) LiPo's, [17] adopt a quadratic model for energy density and perform a battery sensitivity study with linear model of variations about a nominal value of 180Wh/kg.

The described endurance model is based on an ideal battery run-time model, which delivers its nominal capacity irrespective of the discharge rate [18]. In practice, the actual capacity delivered by the battery depends on the discharge rate [15], and [2], [18]–[20] highlight the importance of accounting for this first-order Capacity-Rate Effect. The simplest way is through a constant Capacity Offset, as adopted in [8] and [21], which is typically between 0.8-0.9. Moreover, [18] and [19] introduce a Battery Efficiency Factor which varies with discharge rate. One of the most widely adopted models considering the Capacity-Rate Effect is the Peukert Equation, an empirical model based on the Peukert Exponent. This is a constant which depends on the battery chemistry as well as its State of Health (SoH), with a value closer to unity signifying an ideal battery [22]. However, [22] and [23] show that the Peukert Equation is not suitable for LiPo's since it is only valid over a limited working range with constant discharge rate and temperature, and the Peukert Exponent also varies with temperature, discharge rate and cycle life. [20] highlights the difference in endurance estimates for a battery-powered aircraft when considering the Peukert effect as compared to an ideal battery, with experimental validation of these calculations presented in [24].

*This work is carried out by the University of Bristol in affiliation with the Bristol Robotics Laboratory and is supported by the Defence Science and Technology Laboratory

[1]PhD Candidate analiza.abdilla@bristol.ac.uk
[2]Reader arthur.richards@bristol.ac.uk
[3]Reader stephen.burrow@bristol.ac.uk

II. ROTORCRAFT POWER MODEL

This section presents a combination of analysis and testing to derive a model of electrical power consumption for a generic rotorcraft in general flight, as a function of its All Up Weight (AUW). This model, together with the battery model derived in Section III, will be used to predict flight endurance with different batteries.

A. Analysis of Hover Power

According to Momentum Theory [9], the rotor hover power P_r $[W]$ is

$$P_r = \frac{T_r^{\frac{3}{2}}}{\eta_r r_p \sqrt{2\rho_a \pi}} \tag{1}$$

where T_r is the rotor thrust, ρ_a is the density of air, r_p is the propeller blade radius, and η_r is a Figure of Merit characterising the rotor's efficiency. Assuming steady hover, $T = mg$, (see Section II-B), the power for a rotorcraft with N_R rotors can thus be derived by considering the total weight to be divided equally between the rotors, as follows:

$$P_{N_R-rotorcraft} = \frac{g^{\frac{3}{2}}}{\eta_{ps} r_p \sqrt{2N_R \rho_a \pi}} m^{\frac{3}{2}} \tag{2}$$

where g is the standard acceleration due to gravity, m is the mass, and η_{ps} is the rotorcraft propulsion system efficiency. This parameter is rotorcraft-specific and is also sensitive to the vehicle's SoH, thus requiring experimental determination. An estimate may be derived based on the rotorcraft scale, where η_{ps} decreases significantly with decreasing rotorcraft size due to the reduction in rotor efficiency as well as the increased interference between rotors [9].

B. Dependence of Power on Manoeuvring

The power consumption of rotorcraft was characterised by measuring the power of the ARDrone2.0 during flight tests at a range of AUW varying between 495 and 570g whilst performing different manoeuvres. These include lateral/translational, vertical and hover, at different altitudes varying between 1.5-2.5m, with various set-points being issued every 10 seconds through a Simulink controller program. Power measurement was achieved using an on-board custom-made voltage and current sensing circuit comprising a sensing resistor for accurate four-terminal sensing, interfacing with an off-the-shelf NI-USB-6211 Data Acquisition kit sampling at 2 samples/second, through signal conditioning circuitry, via 5m of lightweight Shielded Twisted Pair cable. Whilst the tether may affect the flight dynamics, such a set-up is sufficient for the purpose of investigating the vehicle's power consumption whilst performing different flight manoeuvres as compared with hover.

As can be observed from the selection of tests displayed in Fig. 1, the power profile for translational and vertical manoeuvres is similar to that for hover at the corresponding mass. This leads to the adoption of hover as the nominal flight regime. Additionally, it can be observed that the power consumption decreases over time, with the magnitude of this decrease depending on the respective AUW. This effect is further investigated and discussed in Section II-D.

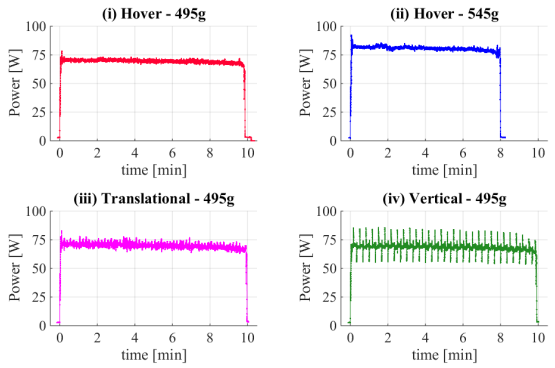

Fig. 1. Power Profiles of ARDrone2.0 for the following flight tests: i) hover at 2m at 495g; ii) hover at 2m at 545g; iii) translational manoeuvres with 5 set-points at 2m at 495g; iv) vertical manoeuvres with 2 set-points at 1.5m and 2m at 495g.

C. Determining the Efficiency

In order to determine the propulsion system efficiency of the ARDrone2.0, its power consumption was measured during hover flight tests at a range of AUW varying between 436 and 577g, using an Off-The-Shelf data logger, namely the eLogger V4 [25], configured for voltage and current acquisition at 10 samples/second. For the ARDrone2.0 quadrotor, $N_R = 4$ and $r_p = 0.102m$. Taking $g = 9.81m/s^2$ and $\rho_a = 1.20kg/m^3$, the power equation (2) can be rearranged to give the efficiency from the measurements. Fig. 2 shows the calculated efficiencies, averaged for each flight, as a function of AUW. The plot suggests a small increase in efficiency with AUW, consistent with the presence of a constant power drain, although a constant efficiency gives a similar quality of fit. Different models will be compared in Section II-E.

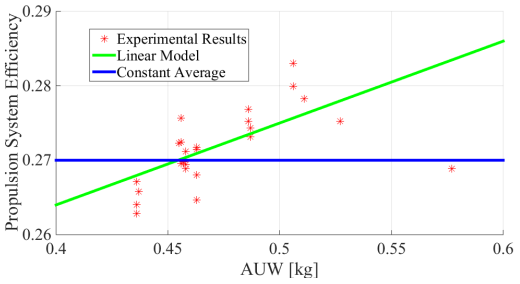

Fig. 2. Variation of ARDrone2.0 Propulsion System Efficiency with AUW.

D. Variation of Efficiency with Voltage

The decrease in electrical power during flight tests at a fixed AUW, as displayed in Fig. 1, indicates improving efficiency over the course of a flight. Two competing hypotheses were formed for this effect: (i) a mechanical change, such as reduction in friction due to heating; or (ii) an electrical effect, such as improved power conversion efficiency at lower battery voltage. Fig. 3 shows the variation in power level during two tests with the ARDrone2.0 supplied by a bench power supply, from which the voltage is first decreased and

then increased again. The drone was clamped down for this test and the control code was overriden to command a constant rotor speed throughout the test. Although clamping and ground effect will affect the power measurements, the test is sufficient to distinguish between the two hypotheses above. Fig. 3 shows that the original power level is recovered as the voltage increases, indicating that the change in efficiency is predominantly due to electrical effects. Fig. 4 shows the power as a function of voltage from the same tests. Aside from an initial transient, these results suggest a roughly linear relationship between supply voltage and power system efficiency.

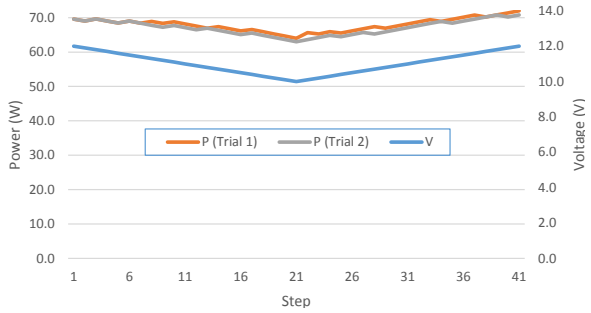

Fig. 3. Variation in electrical power with decreasing and increasing voltage from a bench power supply for a clamped ARDrone2.0 at a constant rotor speed.

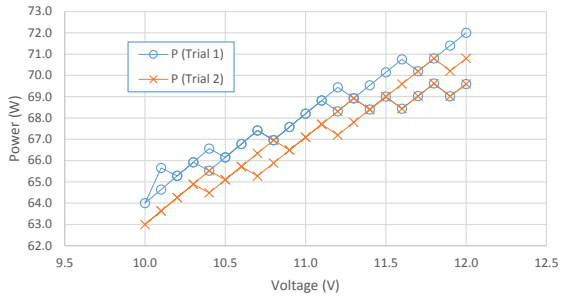

Fig. 4. Power variation with voltage for the clamped ARDrone2.0 at a constant rotor speed.

E. Comparison of Power Models

The most complete power model suggested by the preceding Sections is in the form

$$P = P_0 + (k_0 + k_V V)m^{\frac{3}{2}} \tag{3}$$

where P_0 is a constant parasitic power loss and (k_0, k_V) represent the momentum theory model (2) with a voltage-dependent efficiency. To test this model, 27 flights were performed at different AUW with the power and voltage logging as described in Section II-C. Data from two of the flights were used to determine coefficients ($P_0 = 13.7, k_0 = 74.5, k_V = 8.00$) for power in W and mass in kg. Validating against the remaining 25 flights, the standard deviation of power was $3.20W$, or roughly 5% of the flight power. Note that the model was found to be sensitive to the individual drone: tests with a different, but also brand new, ARDrone2.0 found values of P_0 and k_V differing by 100% from those above.

For comparison, a simplified model was evaluated based purely on the momentum theory model (2) with constant efficiency and no loss term:

$$P = k_a m^{\frac{3}{2}} \tag{4}$$

Using the same flight test data as above, the coefficient $k_a = 200$ was determined, giving a standard deviation of $3.59W$, worse than the detailed model but still less than 10% of the hover power. Although in some circumstances that could be considered a large error, it will be shown in Section III that battery variability dominates power uncertainty for endurance prediction. Furthermore, the simpler model (4) was found to be significantly less sensitive to the individual ARDrone2.0 used.

F. Effect of Motor Controller Saturation

Fig. 5 shows the results of further experiments with a clamped ARDrone2.0. Hovering at a range of AUW was simulated by directly controlling the rotor speeds, overriding the built-in code with direct speed commands. For these tests, the ARDrone was powered from a bench power supply with a range of voltages corresponding to those of 3S LiPo voltages, namely between 12.6 and 9V. The input voltage was decreased over this range to simulate the battery's terminal voltage during discharge. It can be observed that at motor speed commands exceeding 360, the power against voltage profiles are comprised of two regimes: "high voltage", where power depends only slightly on voltage; and "low voltage", where electrical power falls away sharply with decreasing voltage. Direct measurement of rotor speeds indicate loss of mechanical power in the low voltage region.

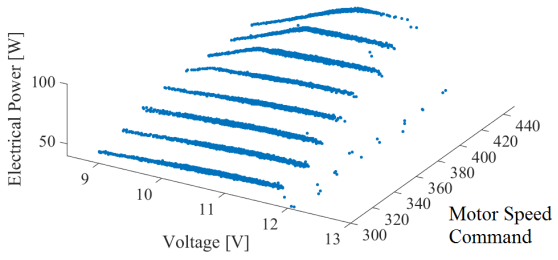

Fig. 5. ARDrone2.0 Electrical Power against Voltage profiles at various motor speed commands

Observation of the motor current waveforms at the maximum and minimum voltage levels, displayed in Fig. 6, indicates the pulse width modulation (PWM) control of current is saturated in the low voltage regime. The threshold voltage for the transition to the saturation region increases with motor speed command and thus AUW, representing a surface of constant modulation at full duty-cycle of the PWM controller. This effect necessitates increasing the minimum voltage threshold for battery discharge with AUW so as to

ensure stable operation, correspondingly reducing the "usable" battery capacity, and resulting in reduced endurance, as discussed in Section IV.

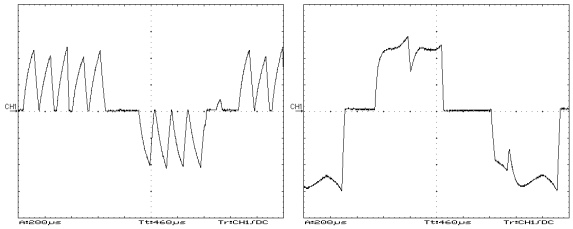

Fig. 6. ARDrone2.0 motor currents at maximum and minimum voltage respectively at a motor speed command of 360.

III. LiPo BATTERY MODELS

A. Experimental Procedure

COTS LiPo batteries were characterised through experiments on a battery test-rig implemented as a Hardware-in-the-Loop (HIL) model of the ARDrone, in order to reduce the resources required for carrying out flight tests and minimise the associated sources of variability and "wear-and-tear". This constructed model is comprised of a carbon-pile resistor emulating the ARDrone's power model via closed-loop control by means of an electronic circuit interfacing with dSPACE.

A selection of the three-cell (3S) LiPo's of various brands and nominal capacities and discharge rates listed in Table I, namely P450, P500, H850, Z850, T1300, H2600 and P2650, were utilised for this purpose. Tests were repeated three times so as to ensure repeatability, with four batteries of each type in order to investigate the inherent variability between batteries. A rigorous testing procedure was adopted, subjecting batteries to a charging regime one day prior to running the discharge test, in order to simulate operational conditions. Batteries were discharged down to the minimum permissible cut-off voltage (3V/cell for LiPo's) at various rates, whilst recording the discharge profiles to enable estimation of the battery run-time and actual delivered capacity.

TABLE I
BATTERY DATA

Nominal Capacity C_{nom} [mAh]	Brand	Mass m_b [g]	Reference
450	Polypower	47	P450
500	Polypower	51	P500
850	Hyperion	72	H850
850	Zippy	75	Z850
1000	Turnigy	78	T1000
1100	Turnigy	93	T1100
1300	Turnigy	112	T1300
2000	Turnigy	153	T2000
2200	Turnigy	191	T2200
2600	Hyperion	223	H2600
2650	Polypower	225	P2650

B. Run-Time Model

Battery run-time experimental results were compared with predictions based on four battery run-time models:

1) Ideal battery: $t = \frac{C_{nom}}{I}$;
2) Capacity Offset $C_o = 0.8$: $t = 0.8\frac{C_{nom}}{I}$;
3) Capacity Offset $C_o = 0.9$: $t = 0.9\frac{C_{nom}}{I}$;
4) Peukert Equation: $t = \frac{{C_{nom}}^{n_P} R_{nom}^{(n_P-1)}}{I^{n_P}}$, with Peukert Exponent $n_P = 1.01$, which is the average value calculated over all the experiments carried out.

Fig. 7 shows that run-time estimates which are closest to experimental results are obtained from the model accounting for the Capacity-Rate Effect through a constant Capacity Offset $C_o = 0.9$. Thus, the battery run-time model adopted is:

$$t[h] = 0.9\frac{C_{nom}[Ah]}{I[A]}. \quad (5)$$

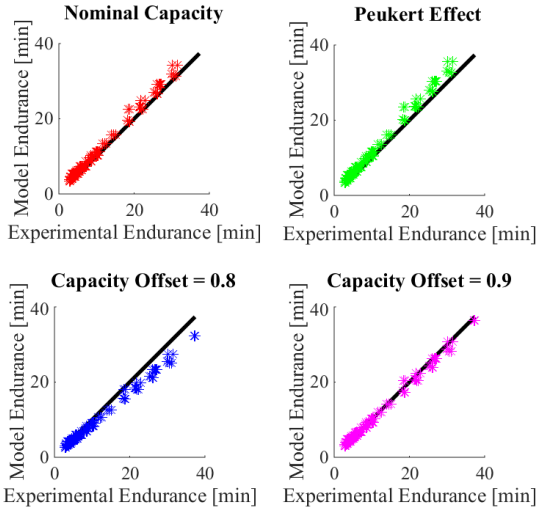

Fig. 7. Battery Run-time Models compared with Experimental Results.

C. Specific Capacity and Energy Models

Experimental results of the actual capacity delivered by these LiPo batteries, displayed in Fig. 8, indicate a linear variation with battery mass. In view of this, the following linear models were adopted for battery capacity and energy respectively:

$$C_{nom}[Ah] = 14.4m_b[kg] - 0.14 \quad (6)$$

$$\Rightarrow E_{nom}[Wh] = C_{nom}V_{nom} = 160m_b[kg] - 1.6 \quad (7)$$

where the nominal voltage $V_{nom} = 11.1V$ for 3S LiPo's.

D. Available Capacity Factor

Experimental results highlight the significance of battery variability, which may be attributed to manufacturing differences as well as the battery SoH, including the effects of cycling history, ageing, and storage and environmental

conditions. This is taken into account in battery models through the introduction of a Battery Available Capacity Factor, k_B. This is characterised by considering the minimum battery capacity during its life-time to be 80% [15], beyond which the battery is typically retired, and thus, the actual capacity of the battery during its life-time is considered to vary between 80-100% of its rated nominal value, i.e., $C_{actual} = k_B C_{nom}$, where k_B is in the range 0.8 to 1.0.

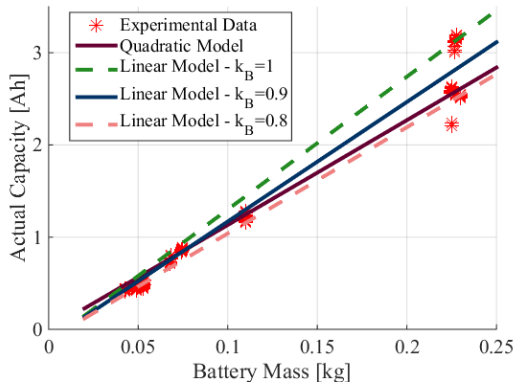

Fig. 8. Battery actual capacity against battery mass: experimental results, quadratic model presented in [17], and adopted linear model accounting for battery variability.

IV. ROTORCRAFT ENDURANCE MODEL

A. General Endurance Model

Given that energy is the product of average power and time, a prediction of endurance can be derived from the simplified average power model (4). This is modified by the inclusion of a usable capacity factor $C_{usable} = k_u(m)C_{actual}$ to account for the controller saturation effect described in Section II-F, which prevents batteries being used beyond a minimum voltage threshold at high power levels. The resulting endurance model is:

$$t = \frac{k_u\left(m\right) k_B C_{nom} V_{nom}}{k_a m^{3/2}} \tag{8}$$

Introducing the LiPo battery specific capacity model (6) enables generalisation of the endurance model to:

$$t = \frac{k_u\left(m\right) k_B \left(160\left[m - m_d\right] - 1.6\right)}{k_a m^{3/2}} \tag{9}$$

where all masses are now in kg and m_d is the rotorcraft "dry" mass, that is, without any batteries, such that $m_d = m - m_b$. Including the calculated coefficient value $k_a = 200$ and the ARDrone2.0 dry mass $m_d = 0.36kg$ with the indoor hull fitted, the endurance model is given by:

$$t_{ARDrone}[h] = 7.8 \times 10^{-3} k_u\left(m\right) k_B \frac{100m - 37}{m^{\frac{3}{2}}} \tag{10}$$

B. Usable Capacity Factor Model

As can be observed from the experimental results displayed in Fig. 9, the actual capacity delivered by the battery may be considered to be 90% ($\pm$ 10% to account for battery variability) up to a mass of $\sim$0.525kg, beyond which it decays rapidly. The Usable Capacity Factor may thus be defined by normalising against the nominal actual capacity (90%) as follows:

$$k_u\left(m\right) = \begin{cases} 1, & m \leq 0.525kg \\ -17.2m^2 + 16.7m - 3, & \text{otherwise} \end{cases}$$

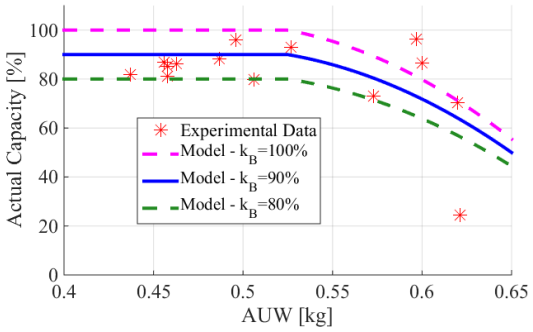

Fig. 9. Battery Actual Capacity against AUW

C. Model Validation

This derived endurance model was validated by performing flight tests on five ARDrones using the batteries listed in Table I. Experimental endurance results, which together with the endurance model (10) are displayed in Fig. 10, result in a maximum absolute error of 1.1 minutes (27.6%) as compared with the model nominal case (8) within an AUW of 550g. Furthermore, a maximum endurance of 16.8-18.5mins is obtained at an AUW of $\sim$550g using a T2200 battery. Note that the endurance prediction reaches a maximum before reducing again with increased mass. This effect is caused by the PWM saturation effect. It should also be noted that flights at an AUW exceeding 550g exhibited unstable behaviour, attributed to the onset the PWM saturation.

V. CONCLUSION

This paper derives and validates an endurance model for electric rotorcraft powered by LiPo batteries. Flight tests characterising rotorcraft power consumption indicate minimal difference for vertical and/or translational flight manoeuvres when compared with hover at the corresponding mass, thus leading to the adoption of hover as the nominal flight regime. A simple rotorcraft power model is derived based on Momentum Theory, with a constant propulsion system efficiency.

At a constant All Up Weight, the electrical power decreases over the course of the flight due to an increase in the electronic switching circuit efficiency with decreasing voltage. Additionally, the saturation of the motor controllers results in unstable operation below a threshold voltage level which depends on the AUW. This results in a corresponding reduction in the "usable" battery capacity and thus endurance. As a result, there is an optimal value of mass which results in maximum endurance, beyond which any additional

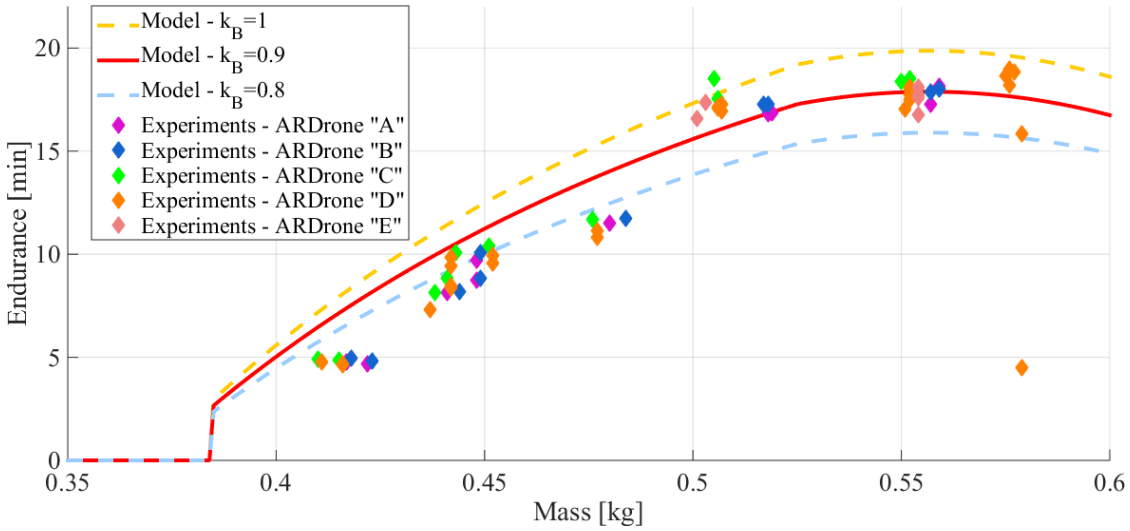

Fig. 10. ARDrone2.0 Endurance: Model accounting for battery variability together with Experimental Results for Stable Operation. Flights at an AUW exceeding 550g exhibited unstable behaviour which frequently necessitated manual landing prior to vehicle autolanding.

battery mass constitutes parasitic on-board mass as it does not translate into increased endurance.

Experiments with COTS LiPo batteries were also carried out to characterise the run-time and specific capacity/energy models, as well as investigate battery variability and cycling effects. These models were combined with the rotorcraft power model considering the electric propulsion system effects to provide an endurance model, which was experimentally validated through flight tests.

REFERENCES

[1] Schmidt, Michael David. "Simulation and Control of a Quadrotor Unmanned Aerial Vehicle." (2011).

[2] Mulgaonkar, Yash, Michael Whitzer, Brian Morgan, Christopher M. Kroninger, Aaron M. Harrington, and Vijay Kumar. "Power and weight considerations in small, agile quadrotors." In SPIE Defense+ Security, pp. 90831Q-90831Q. International Society for Optics and Photonics, 2014.

[3] Abdilla, Analiza, Richards, Arthur, Burrow, Stephen, "Endurance Optimisation of Battery-Powered Rotorcraft". Towards Autonomous Robotic Systems, Springerlink, 2015.

[4] PARROT ARDrone2.0 Web-site http://ardrone2.parrot.com/

[5] Beekman, Daniel W. "Micro air vehicle endurance versus battery size." In SPIE Defense, Security, and Sensing, pp. 767910-767910. International Society for Optics and Photonics, 2010.

[6] Whitney, J. P., and R. J. Wood. "Conceptual design of flapping-wing micro air vehicles." Bioinspiration & Biomimetics 7, no.3 (2012):036001.

[7] Neitzke, Klaus-Peter. "Rotary Wing Micro Air Vehicle Endurance." In Proceedings of the International Micro Air Vehicle Conference and Flight Competition IMAV. 2013.

[8] Mulgaonkar, Yash, and Vijay Kumar. "Autonomous charging to enable long-endurance missions for small aerial robots." In SPIE Defense+ Security, pp. 90831S-90831S. International Society for Optics and Photonics, 2014.

[9] Leishman, J. Gordon. "Principles of Helicopter Aerodynamics. 2006." Cambridge Aerospace Series.

[10] Andres. Optimal battery capacity. Technical report, 2011.

[11] Wagner, N., S. Boland, B. Taylor, D. Keen, J. Nelson, and T. Bradley. "Powertrain design for hand-launchable long endurance unmanned aerial vehicles." 2012-01-01]. http://www. engr. colostate. edu/-thb/Publications/SD UAV Final No Markup.pdf (2011).

[12] Lawrence, Dale A., and Kamran Mohseni. "Efficiency analysis for long-duration electric MAVs." American Institure of Aeronautics and Astronautics Infotech, AIAA 2005 7090 (2005).

[13] Harrington, Aaron M., and Christopher M. Kroninger. "Endurance bounds of aerial systems." In SPIE Defense+ Security, pp. 90831R-90831R. International Society for Optics and Photonics, 2014.

[14] Roberts, James F., J-C. Zufferey, and Dario Floreano. "Energy management for indoor hovering robots." In Intelligent Robots and Systems, 2008. IROS 2008. IEEE/RSJ International Conference on, pp. 1242-1247. IEEE, 2008.

[15] Dell, Ronald M., and David Anthony James Rand. Understanding batteries. Royal Society of Chemistry, 2001.

[16] Battery Ragone Plot http://www.iccnexergy.com/battery-systems/battery-energy-density-comparison/

[17] Gur, Ohad, and Aviv Rosen. "Optimizing electric propulsion systems for unmanned aerial vehicles." Journal of aircraft 46, no. 4 (2009): 1340-1353.

[18] Park, Sung, Andreas Savvides, and Mani Srivastava. "Battery capacity measurement and analysis using lithium coin cell battery." In Proceedings of the 2001 international symposium on Low power electronics and design, pp. 382-387. ACM, 2001.

[19] Pedram, Massoud, and Qing Wu. "Design considerations for battery-powered electronics." In Proceedings of the 36th annual ACM/IEEE Design Automation Conference, pp. 861-866. ACM, 1999.

[20] Traub, Lance W. "Range and endurance estimates for battery-powered aircraft." Journal of Aircraft 48, no. 2 (2011): 703-707.

[21] Stepaniak, Michael J., Frank Van Graas, and Maarten Uijt De Haag. "Design of an electric propulsion system for a quadrotor unmanned aerial vehicle." Journal of Aircraft 46, no. 3 (2009): 1050-1058.

[22] Omar, Noshin, Peter Van den Bossche, Thierry Coosemans, and Joeri Van Mierlo. "Peukert Revisited–Critical Appraisal and Need for Modification for Lithium-Ion Batteries." Energies 6, no. 11 (2013): 5625-5641.

[23] Doerffel, Dennis, and Suleiman Abu Sharkh. "A critical review of using the Peukert equation for determining the remaining capacity of lead-acid and lithium-ion batteries." Journal of power sources 155, no. 2 (2006): 395-400.

[24] Traub, L. W. "Validation of endurance estimates for battery powered UAVs." Aeronautical Journal 117.1197 (2013): 1155-1166.

[25] EagleTree eLogger `http://www.eagletreesystems.com/index.php?route=product/product&product_id=54`